J. S. Artal-Sevil, J. Anzola, V. Ballestín-Bernad and I. Aizpuru, "Bidirectional Cuk Converter in Partial-Power Architecture with Current Mode Control for Battery Energy Storage System in Electric Vehicles," 2022 24th European Conference on Power Electronics and Applications (EPE'22 ECCE Europe), 2022, pp. 1-9.

Bidirectional Cuk Converter in Partial-Power Architecture with Current Mode Control for Battery Energy Storage System in Electric Vehicles

J.S. Artal-Sevil[1], J. Anzola[2], V. Ballestín-Bernad[1], I. Aizpuru[2]
[1]Department of Electrical Engineering.
Polytechnic School of Engineering and Architecture, EINA.
University of Zaragoza. Spain.
[2]Electronics and Computer Science Department.
Goi Eskola Politeknikoa-Orona Ideo-Fundazioa eraikina
Mondragon Unibertsitatea. Spain.
E-mail: {jsartal, ballestin}@unizar.es, {janzola, iaizpuru}@mondragon.edu

Acknowledgements

The authors would like to thank the support of Government of Aragon and the European Union for the project T28_20R, "building Aragon from Europe". This work was supported in part by the Spanish MINECO under Grant RTC-2015-3358-5. The authors also want to thank the support of the IDI project, "study and analysis of partial-power processing architectures for the development of an on-board charger in electric and hybrid vehicles" with reference OTRI-2020/0416.

Keywords

«Partial-Power Processing Converter (PPC)», «non-isolated bidirectional Partial-Power architectures», «DC-DC switched-mode power supplies», «high power», «DC-fast charges», «battery energy storage system (BESS)», «on-board charger».

Abstract

This paper presents a partial-power processing architecture intended for an on-board charger. This module is integrated into a Battery Energy Storage System (BESS). This model allows us to easily control the charge-discharge current of the $LiFePO_4$ battery, as well as the current injection on the DC-bus (V2G). The architecture used in the partial-power processing is based on the non-isolated bidirectional Cuk converter, with average current mode control. The purpose has been to compare both topologies, Full-Power and Partial-Power, to observe the advantages and disadvantages that each on-board charger design offers. Partial architecture has some advantages such as high power density, small size, decrease stress on devices, as the DC-DC converter only processes a fraction of the total power. Thus, the purpose of this paper has been to analyze and explore the usefulness of the non-isolated bidirectional Cuk converter with partial-power processing architecture in battery charging systems in electric vehicles. The effectiveness of the strategy has been validated by the *Matlab/Simulink* software simulation.

1. Introduction

The incorporation of the partial-power philosophy allows us to use smaller and cheaper converters since power losses are reduced. These design concepts are an attractive solution and have attracted the attention of the research community in recent years [1]. The full-power converter processes all the energy supplied to the load, while the partial-power converter only processes a fraction of the power.

This architecture has already been implemented in numerous applications, such as the integration of photovoltaic systems [2] [3], battery charging systems in electric vehicles [4], DC-power supply [5], active balancing of PV-arrays [6] or MPPT search algorithms in TEG systems [7], spacecraft [8], etc., in order to improve system performance. In short, the partial converter can improve the efficiency of the entire system while reducing its cost. It is an advantage of this architecture. Although, there are also opinions that doubt the performance improvement in non-isolated topologies [9].

This partial-power topology is being implemented in higher power applications. As an example, Iyer *et al.* [4], [10] propose a fast-charging station for different battery electric vehicles (BEV) and plug-in hybrids (PHEV) based on partial-power processing architecture. Likewise, Xue *et al.* [11] and Artal-Sevil *et al.* [12] develop a low-cost bidirectional fractional DC-DC converter, intended for a high-power battery energy storage system (BESS). Its main objective was to reduce the power processed by the converter, in order to increase the overall efficiency of the system. While Anzola *et al.* [13] describe a charging unit based on partial-power processing for extremely fast charging stations for electric vehicles. Similarly, Mira *et al.* [14] present the analysis of a DC-DC mode switching power supply in a partial-power processing configuration. The presented model is based on the Dual Active Bridge (DAB) architecture and constitutes a unidirectional charge converter. This topology is also being used in systems that introduce energy storage systems. In [15] a partial-power processing architecture for a hybrid electric vehicle (HEV) based on Fuel-Cells is presented. The supply system includes an active buffer, in partial-power topology, to supply the power peaks demanded by the vehicle's traction.

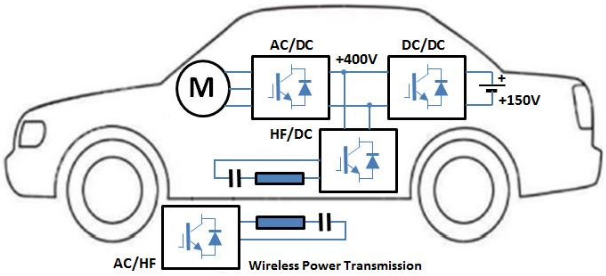

Fig. 1. On-board charger diagram in a wireless power transfer charging system. Application of the partial-power processing architecture on a non-isolated bidirectional Cuk DCDC converter.

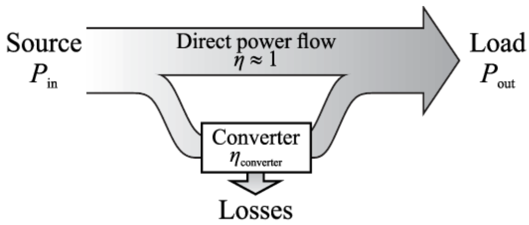

Fig. 2. Concept of power flow in partial-power converter.

On the other hand, vehicle to grid (V2G) is an emerging technology that is being analyzed for electric vehicles (EV), see Fig. 1. The energy stored in battery packs can be an alternative to power demand peaks on the grid [16]. This technology requires the development of smart on-board chargers, integrated into the vehicle, that have the ability to manage the power flow [17] [18]. This paper proposes partial-power processing architecture for the design of a smart on-board charger. The main objective is to validate the advantages of the partial-power architecture in these applications. For this purpose, multiple simulations have been carried out in *Matlab-Simulink*. Likewise, in [19] [20] the design of a high-density battery charger with different converter architectures based on partial-power processing has been described. These designs stand out for their high efficiency.

This paper is organized as follows. Section 1 shows a brief introduction associated with the problem addressed. Section 2 presents the mathematical analysis of the partial-power converter. Section 3 provides a description of the system configuration. Section 4 shows the different simulation results obtained with the *Matlab-Simulink* software. Finally, the conclusions and some brief considerations are described in Section 5.

2. Proposed Cuk Converter in Partial-Power Processing Architecture

In Fig. 2 the concept of power flow in partial-power architecture is shown. The proposed converter has been derived from the classic Cuk converter. To simplify the steady-state analysis of the proposed architecture, some assumptions are made, such as ideal switching devices and inductors, with no delay in the switching process. For a sampling time T_{SW}, the switch is ON for $D \times T_{SW}$ and OFF for the period $(1 - D) \times T_{SW}$. Therefore, depending on the state of the switch, two modes of operation can be identified.

Mode 1: ON-state $[0 \leq t \leq D(t) T_{SW}]$.

At the initial time t = 0, when switch SW_1 turns on, diode D_1 turns off. The inductor currents (i_{L1}, i_{L2}) increase from their respective initial value. The voltage and current equations are as follows:

$$v_{L1}(t) = L_1 \frac{\partial i_{L1}}{dt} = v_G \; ; \quad v_{L2}(t) = L_2 \frac{\partial i_{L2}}{dt} = v_{C1} - v_C \tag{1}$$

$$i_{C1}(t) = C_1 \frac{\partial v_{C1}}{dt} = i_{L2}\,; \quad i_C(t) = C\frac{\partial v_C}{dt} = i_{L2} - i_O \tag{2}$$

$$v_O = v_G - (-v_C) \tag{3}$$

Mode 2: OFF-state [$D(t)T_{SW} \leq t \leq T_{SW}$].

When switch SW_1 turns off at t = D·T$_{SW}$, diode D_1 turns on. A similar analysis gives the equations for voltage and current as follows:

$$v_{L1}(t) = L_1 \frac{\partial i_{L1}}{dt} = v_G - v_{C1}\,; \quad v_{L2}(t) = L_2 \frac{\partial i_{L2}}{dt} = -v_C \tag{4}$$

$$i_{C1}(t) = C_1 \frac{\partial v_{C1}}{dt} = -i_{L1}\,; \quad i_C(t) = C\frac{\partial v_C}{dt} = i_{L2} - i_O \tag{5}$$

The average inductor voltage (v_{L1}, v_{L2}) must be zero at steady-state. Hence, analyzing the volt-sec balance for inductors (L_1, L_2) during a switching period T_{SW}, we obtain:

$$v_{L1}(t) = 0 \rightarrow v_G \cdot D(t) + \{v_G - v_{C1}\} \cdot \{1 - D(t)\} = 0 \tag{6}$$

$$v_{L2}(t) = 0 \rightarrow \{v_{C1} - v_C\} \cdot D(t) - v_C \cdot \{1 - D(t)\} = 0 \tag{7}$$

As input voltage (v_G) is assumed to be constant over a switching period. Solving for steady-state output voltage v_O then,

$$v_O = v_G \frac{1}{1-D} \tag{8}$$

Likewise, the instantaneous value in the duty cycle ratio *D(t)* depends on the input voltage v_G, and can be expressed as

$$D = 1 - \frac{v_G}{v_O} \tag{9}$$

Similarly, the average capacitor current (v_C, v_{C1}) must be zero in steady-state. Hence, analyzing the current-sec balance for the capacitors (C, C_1) during a T_{SW} switching period, we obtain:

$$i_{C1}(t) = 0 \rightarrow i_{L2} \cdot D(t) + (-i_{L1}) \cdot \{1 - D(t)\} = 0 \tag{10}$$

$$i_C(t) = 0 \rightarrow \{i_{L2} - i_O\} \cdot D(t) + \{i_{L2} - i_O\} \cdot \{1 - D(t)\} = 0 \tag{11}$$

Solving for the current in the inductors (i_{L1}, i_{L2}) in steady state then,

$$i_{L1} = i_{L2} \frac{D}{1-D}\,; \qquad i_{L2} = i_O \tag{12}$$

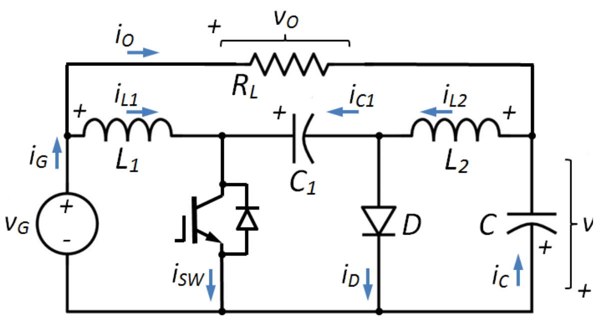

Fig. 3. Cuk converter in partial-power processing architecture.

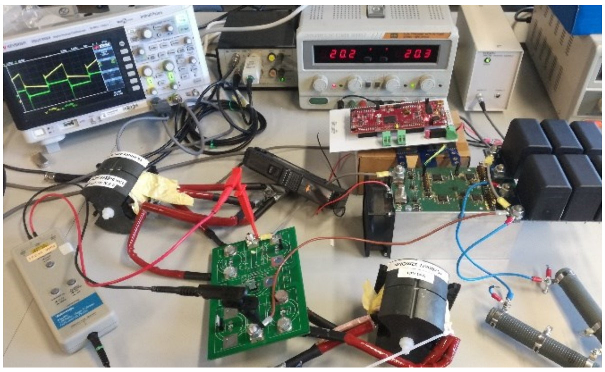

Fig. 4. Experimental testing of the Cuk converter in partial-power processing architecture.

And calculating the current i_G supplied by the voltage source v_G, we obtain (13).

$$i_G = i_{L1} + i_O = i_O \frac{1}{1-D} \tag{13}$$

Also, it is possible to determine the input resistance R_G of the converter. In this case, it is given by,

$$R_G = \frac{v_G}{i_G} = \frac{v_O}{i_O}(1-D)^2 = R_L(1-D)^2 \tag{14}$$

3. On-Board Charger based on Partial-Power Processing Architecture

Traditionally, the load ($LiFePO_4$ battery in this case) is connected to the output (v_C) on the DC-DC converter. In other words, in the full-power structure, this converter processes all the power supplied to the battery from the DC-bus, see Fig. 3. Meanwhile, in the partial-power architecture, the load is connected in series between the DC-bus and the Cuk converter output (v_C). Figure 5 shows the partial-power processing architecture diagram in the Cuk converter. This converter topology is bidirectional, non-isolated, and has two inductors. The charge-discharge current (i_{Li}) in the $LiFePO_4$ battery, or the current injection on the grid (V2G), can be controlled by the duty cycle (D) in the converter.

For example, during the current charging process in the $LiFePO_4$ battery, the G_{vFPC} voltage gain ($G_{vFPC} = v_{OUT}/v_{IN}$) in continuous conduction mode (CCM) for the Cuk converter operating as full-power architecture (FPC), is given by (15). Whereas the G_{vPPC} voltage gain for the Cuk converter operating in partial-power architecture (PPC) is given by (16).

$$G_{vFPC} = \frac{v_O}{v_{IN}} = \frac{v_{Li}}{v_{DC}} = \frac{D}{1-D} \tag{15}$$

$$G_{vPPC} = \frac{v_O}{v_{IN}} = \frac{v_{DC}}{v_{C2}} = \frac{v_{DC}}{v_{DC} - v_{Li}} = \frac{1}{1-D} \tag{16}$$

where v_{IN} is the input voltage and v_O is the output voltage of the Cuk converter in each case; v_{Li} and v_{DC} represent the voltage at the $LiFePO_4$ battery terminals (BESS) and the voltage on the DC-bus respectively, and D is the duty cycle in Cuk converter module.

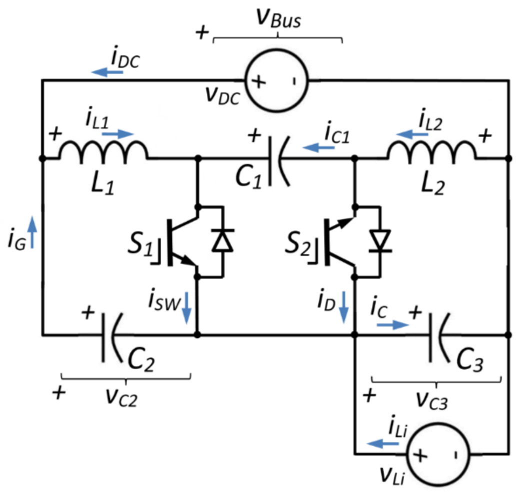

Fig. 5. Schematic diagram of the bidirectional Cuk converter in partial-power processing architecture applied to an on-board charger.

TABLE I. PARAMETERS ASSOCIATED WITH THE BIDIRECTIONAL CUK PARTIAL-POWER CONVERTER MODEL.

Parameter	Symbol	Value
DC-bus voltage	v_{DC}	+150V
Module internal resistance	r_{DC}	0,1Ω
$LiFePO_4$ battery voltage	v_{Li}	+45V to +55V
Internal battery resistance	r_{Li}	0,025Ω
Cuk inductors	L_1, L_2	5mH
Cuk capacitor	C_1	500μF
Switching frequency	f_{SW}	10kHz
Switch resistance S_1, S_2	R_{on}	0,01Ω
Schottky forward voltage	v_F	0,3V
Snubber network	R_S, C_S	10kΩ; 10nF
Input/Output Capacitor	C_2, C_3	500μF

Note that in the full-power topology, the output voltage can be higher or lower than the input voltage as the duty cycle increases (D). Whereas in the partial-power architecture, the output voltage is always higher than the input voltage depending on the value adopted by the duty cycle (D). In this assumption, operating with eq. 16, the relationship between the DC-bus voltage (v_{DC}) and the battery voltage (v_{Li}) is obtained as,

$$v_{DC}(1-D) = v_{DC} - v_{Li}\ ; \quad v_{Li} = D \cdot v_{DC} \tag{17}$$

4. Simulation Results

In order to study the characteristics of a partial-power architecture applied to a battery energy storage system, a non-isolated bidirectional Cuk converter has been modelled in partial-power processing mode.

The analyzed topology is shown in Fig. 5. The simulation software used has been *Matlab-Simulink*. At the same time, an average current mode control has been developed. Likewise, Table I contains some of the parameters used in the development of the model.

Cuk converter in partial-power topology switches at a frequency f_{SW} = 10kHz. This structure uses two coils L_1, L_2 with the value of 5mH, and a capacitor C_1 with the value of 500µF. A small internal resistance in series with each voltage source (r_{DC} = 0,1Ω and r_{Li} = 0,025Ω) represents the power losses during charge/discharge processes in the bidirectional Cuk converter. Figure 6 shows the currents associated with each coil (i_{L1}, i_{L2}) as well as the current i_{Li} during the $LiFePO_4$ battery charging process. The sign of the current i_{Li} is considered negative ($i_{Li} < 0$) during the charging process, while i_{Li} is considered positive ($i_{Li} > 0$) during the $LiFePO_4$ battery discharge process. The signs in the current flows can be seen in the diagram of the Cuk partial-power converter, see Fig. 5.

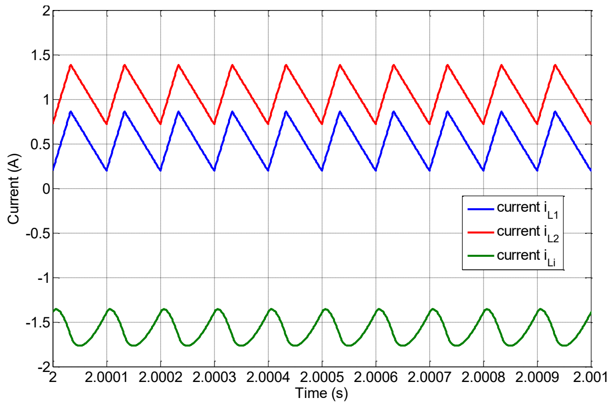

Fig. 6. Steady-state response of the bidirectional Cuk converter in partial-power architecture: current mode control. i_{L1}, i_{L2}, and i_{Li} currents during the $LiFePO_4$ battery charging process (i_{Li} = -1,50A).

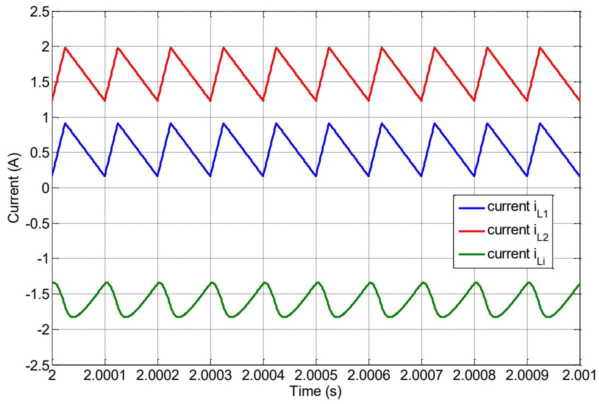

Fig. 7. Steady-state response of the bidirectional Cuk converter in full-power architecture: current mode control. i_{L1}, i_{L2}, and i_{Li} currents during the $LiFePO_4$ battery charging process (i_{Li} = -1,50A).

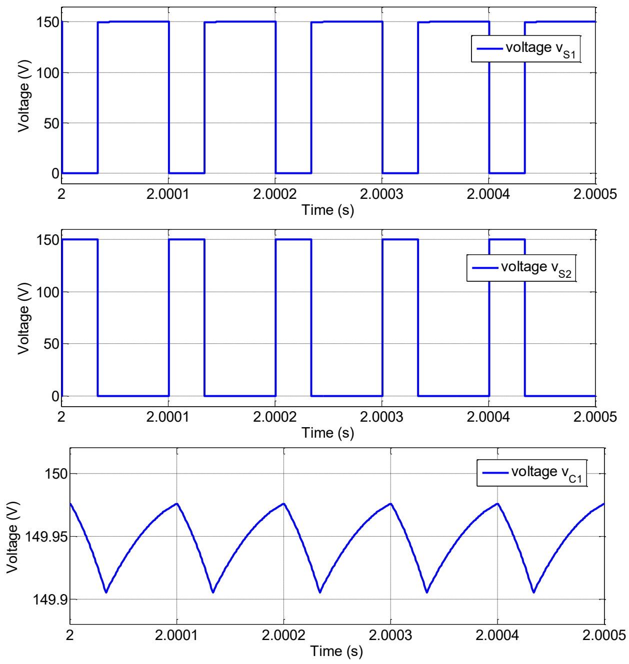

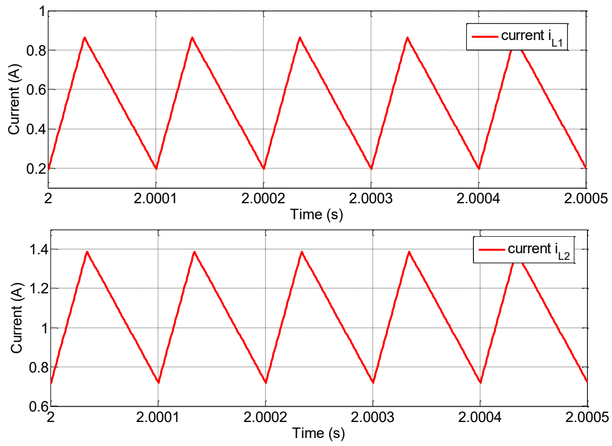

Fig. 8. Steady-state response of the bidirectional Cuk converter in partial-power architecture: v_{S1}, i_{L1}, v_{S2}, i_{L2}, and v_{C1} voltages and currents during the LiFePO4 battery charging process (i_{Li} = -1,50A).

In the Cuk converter in partial-power architecture, with average current mode control, during the battery charging process (i_{Li} = -1,50A) the following average currents are obtained in the inductors: i_{L1} = +0,524A, i_{L2} = +1,042A, see details in Fig. 6. While the current ripple in the inductors corresponds to Δi_{L1} = ±0,334A, Δi_{L2} = ±0,334A. Under these conditions, the capacitor voltage v_{C1} is equal to the DC-bus voltage (v_{DC}), v_{C1} = +150V. In Fig. 7 the currents i_{L1}, i_{L2} corresponding to the Cuk topology coils in full-converter mode are observed. The purpose is to compare the results between both topologies (Cuk partial-converter and Cuk full-converter), considering the same charging current in the $LiFePO_4$ battery.

In this way, it is possible to analyze the advantages provided by the partial-power processing architecture applied to battery energy storage systems (BESS).

In the Cuk converter in full-power architecture, with average current mode control, during the battery charging process (i_{Li} = -1,50A) the following average currents are obtained in the inductors: i_{L1} = +0,5354A, i_{L2} = +1,596A, see details in Fig. 7. While the current ripple in the inductors corresponds to Δi_{L1} = ±0,375A, Δi_{L2} = ±0,375A. Under these conditions, the capacitor voltage v_{C1} is not similar to the DC-bus voltage (v_{DC}), v_{C1} = +200V. In this case, the duty cycle for the Cuk full-power topology is $D_{S1}|_{FP}$ = 0,2502. In view of the simulation results, the stress on the different devices is higher in the full-power converter than in the partial-power converter for the same requested power, see Figs. 6 and 7.

Figure 8 represents the different voltages (v_{S1}, v_{S2}, and v_{C1}) in the semiconductor devices and capacitor respectively, as well as the currents in the inductors (i_{L1}, i_{L2}) of the Cuk converter in partial-power architecture during the current charging process in $LiFePO_4$ battery. Under these conditions, the following values were obtained: DC-bus voltage v_{DC} = +150V, capacitor voltage C_2 (v_{C2} = +99,91V), average DC-bus current i_{DC} = 0,5239A, while the average current and voltage in the $LiFePO_4$ battery (i_{Li}, v_{Li}) are i_{Li} = 1,565A, v_{Li} = +50,04V, respectively. In this case, for the Cuk partial-power architecture, the duty cycle results $D_{S1}|_{PP}$ = 0,3338.

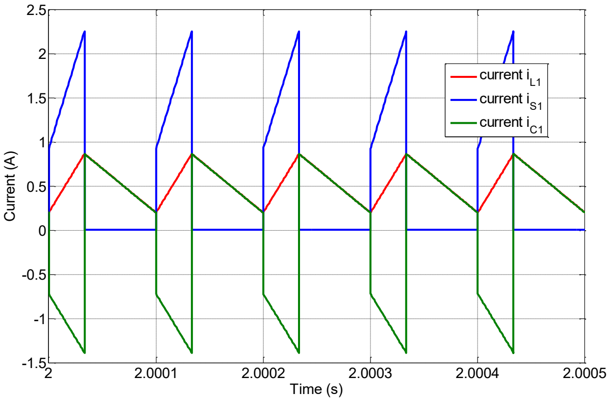

Fig. 9. Steady-state response of the bidirectional Cuk converter in partial-power architecture: i_{L1}, i_{S1}, and i_{C1} currents during the $LiFePO_4$ battery charging process (i_{Li} = -1,50A).

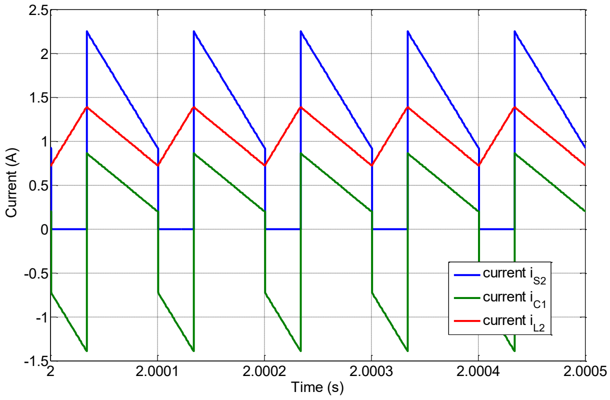

Fig. 10. Steady-state response of the bidirectional Cuk converter in partial-power architecture: i_{L2}, i_{S2}, and i_{C1} currents during the $LiFePO_4$ battery charging process (i_{Li} = -1,50A).

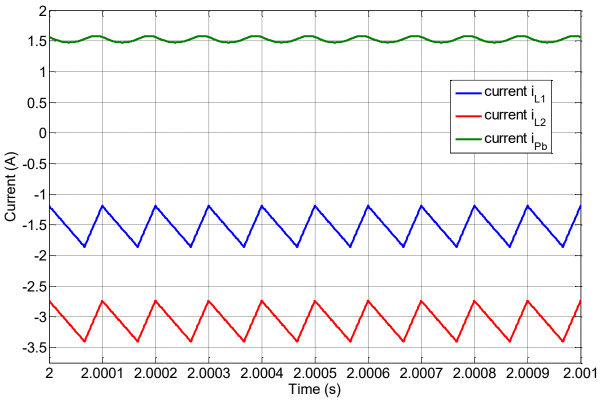

Fig. 11. Steady-state response of the bidirectional Cuk converter in partial-power architecture: current mode control. i_{L1}, i_{L2}, and i_{DC} currents during the LiFePO4 battery discharging process. Power flow goes from $LiFePO_4$ battery to DC-bus (i_{DC} = +1,50A); vehicle-to-grid (V2G) operation.

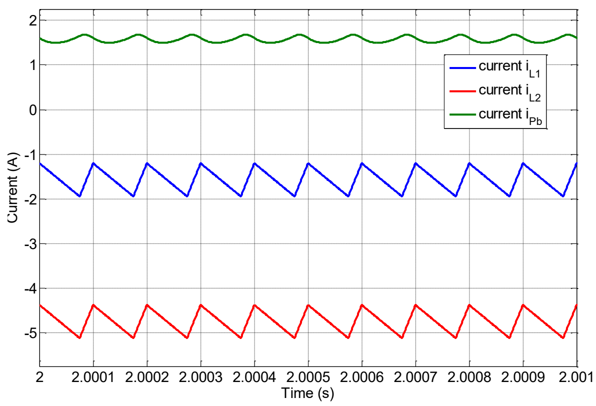

Fig. 12. Steady-state response of the bidirectional Cuk converter in full-power architecture: current mode control. i_{L1}, i_{L2}, and i_{DC} currents during the LiFePO4 battery discharging process. Power flow goes from $LiFePO_4$ battery to DC-bus (i_{DC} = +1,50A); vehicle-to-grid (V2G) operation.

Figure 9 shows the current waveforms in the inductor L_1 (i_{L1}), switch S_1 (i_{S1}), and the capacitor C_1 (i_{C1}), during the $LiFePO_4$ battery charging process. Similarly, applying Kirchhoff's law to the initial node (see Fig. 5), we obtain:

$$i_{L1}(t) = i_{S1}(t) + i_{C1}(t) \tag{18}$$

While in Fig. 10 the current waveforms in the inductor L_2 (i_{L2}), switch S_2 (i_{S2}), and the capacitor C_1, (i_{C1}), during the LiFePO$_4$ battery charging process, are observed.

$$i_{S2}(t) = i_{L2}(t) + i_{C1}(t) \tag{19}$$

Under these conditions (LiFePO$_4$ battery charging current $i_{Li} = -1{,}50A$), the average value of the current in the different switches (i_{S1}, i_{S2}) is: $i_{S1} = 0{,}524A$; $i_{S2} = 1{,}042A$. Likewise, these values support those obtained in the average currents of the L_1 and L_2 converter coils.

Similarly, the simulation results corresponding to the bidirectional Cuk converter in partial-power architecture during the LiFePO$_4$ battery discharge process are presented in Fig. 11, that is, the power flow goes from the battery to the DC-bus. This case corresponds to the power flow injection in the DC-bus, vehicle-to-grid (V2G) operation.

Figure 11 shows the currents i_{L1}, i_{L2} corresponding to the inductors of the Cuk converter in partial-power topology together with the current injected into the DC-bus ($i_{DC} = +1{,}50A$). As mentioned above, in the case of the DC-bus, the sign of the i_{DC} current is considered positive ($i_{DC} > 0$) during the power injection process (V2G operation), that is, in the LiFePO$_4$ battery discharge process. Meanwhile, the i_{DC} current is considered negative ($i_{DC} < 0$) during the LiFePO$_4$ battery charging process. See this sign convention on the Cuk converter diagram (Fig. 5).

In the Cuk converter in partial-power architecture, with current mode control, during current injection on the DC-bus ($i_{DC} = +1{,}50A$), the following average currents are obtained in the inductors: $i_{L1} = -1{,}524A$, $i_{L2} = -3{,}062A$, see Fig. 11. Furthermore, the current ripple in the inductors corresponds to $\Delta i_{L1} = \pm 0{,}334A$, $\Delta i_{L2} = \pm 0{,}334A$. Under these conditions, the capacitor voltage v_{C1} is equal to the DC-bus voltage (v_{DC}), $v_{C1} = +150{,}2V$.

In this case the following values were obtained: DC-bus voltage $v_{DC} = +150{,}3V$; capacitor voltage C_2 $v_{C2} = +100{,}3V$ and LiFePO$_4$ battery voltage $v_{Li} = +49{,}89V$. Likewise, the average currents obtained in the DC-bus (i_{DC}) and in the LiFePO$_4$ battery (i_{Li}) were: $i_{DC} = +1{,}524A$, $i_{Li} = +4{,}582A$.

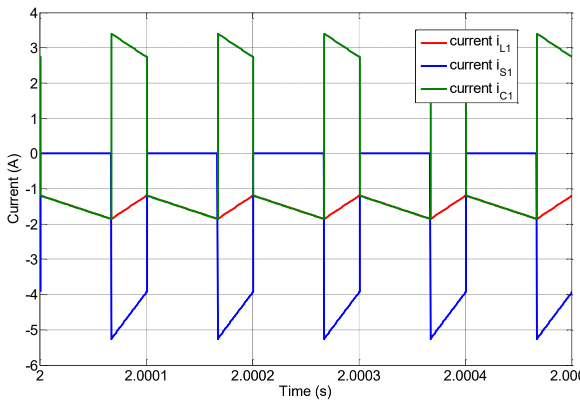

Fig. 13. Steady-state response of the bidirectional Cuk converter in partial-power architecture: i_{L1}, i_{S1}, and i_{C1} currents during the current injection process on the DC-bus. Power flow goes from LiFePO$_4$ battery to DC-bus ($i_{DC} = +1{,}50A$); vehicle-to-grid (V2G) operation.

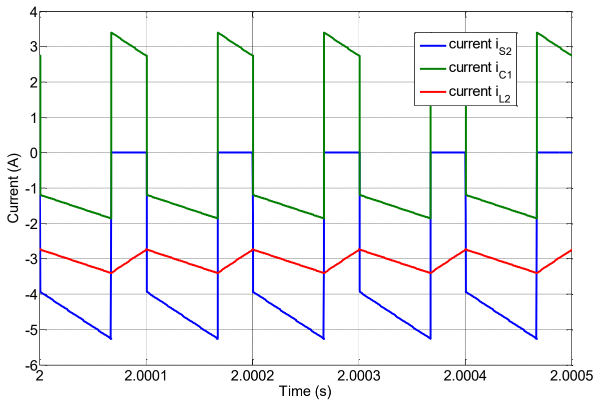

Fig. 14. Steady-state response of the bidirectional Cuk converter in partial-power architecture: i_{L2}, i_{S2}, and i_{C1} currents during the LiFePO4 battery discharging process. Power flow goes from LiFePO$_4$ battery to DC-bus ($i_{DC} = +1{,}50A$); vehicle-to-grid (V2G) operation.

Figure 12 shows the behavior of the bidirectional Cuk converter in the full-power architecture, with control in average current mode, during current injection on the DC-bus ($i_{DC} = +1{,}50A$). In this case, the following average currents were obtained in the inductors: $i_{L1} = -1{,}556A$, $i_{L2} = -4{,}698A$; see details in Fig. 12. While the current ripple in the inductors corresponds to $\Delta i_{L1} = \pm 0{,}375A$, $\Delta i_{L2} = \pm 0{,}375A$. Under these conditions, the capacitor voltage C_1 becomes $v_{C1} = +200V$. Now, in this case, the duty cycle of the Cuk converter in full-power architecture is $D_{S2}|_{FP} = 0{,}7502$. As in the previous assumption, in view of the simulation results obtained in the current injection to the DC-bus, the stress of the devices is higher in the full-power architecture than in the partial-power architecture, considering the same power requirements (see details in Figs. 11 and 12).

Figure 13 shows the current waveforms in inductor L_1 (i_{L1}), switch S_1 (i_{S1}), and capacitor C_1 (i_{C1}) during the current injection process on the DC-bus in partial-power topology. That is, the power flow goes from the $LiFePO_4$ battery to DC-bus (i_{DC} = +1,50A); vehicle-to-grid (V2G) operation. Likewise, Fig. 14 shows the current waveforms in inductor L_2 (i_{L2}), switch S_2 (i_{S2}), and capacitor C_1 (i_{C1}), during this $LiFePO_4$ battery discharge process. Under these conditions, the average current value in the different switches (i_{S1}, i_{S2}) was: i_{S1} = -1,556A; i_{S2} = -4,698A. Now, in this case, the duty cycle of the bidirectional Cuk converter in partial-power architecture is $D_{S2}|_{PP}$ = 0,6679.

5. Conclusions

This paper presents the analysis of a non-isolated bidirectional Cuk converter in partial-power processing architecture. The topology has been applied to an on-board charger in an electric vehicle, supported by the Battery Energy Storage System (BESS). Furthermore, an average current mode control has been developed and implemented in this application. The purpose has been to compare both architectures (full-power and partial-power converter) to validate their advantages in the on-board charger design.

In view of the simulation results obtained, the stress on the different devices is greater in the full-power architecture than in the partial-power architecture, for the same power requirements. In addition, the partial-power topology only processes a fraction of the total power (the voltage difference between the DC-bus and the battery energy storage system), reducing power losses in the overall system. This allows us to reduce the nominal power in the DC-DC converter, with respect to the full-power topology, and at the same time causes a reduction in its cost, volume, and weight.

Finally, the simulation model has been developed with *Matlab-Simulink* software. The control system based on the average current has responded satisfactorily to the charge-discharge current requirements of the $LiFePO_4$ battery, as well as the current injection on the DC-bus.

References

[1] J. Anzola, I. Aizpuru, A. Arruti Romero, A. Alacano Loiti, R. Lopez-Erauskin, J.S. Artal-Sevil and C. Bernal, "Review of Architectures Based on Partial Power Processing for DC-DC Applications" IEEE Access. IEEExplore Digital Library. Vol. 8, June 2020. pp.: 1-14.

[2] J.R.R. Zientarski, M.L. da Silva, J. Renes Pinheiro and H. Leães Hey, "Evaluation of Power Processing in Series-Connected Partial-Power Converters". IEEE Journal of Emerging and Selected Topics in Power Electronics. IEEExplore Digital Library. Vol.: 7, issue: 1, March 2019; pp. 343–352.

[3] J.W. Zapata, S. Kouro, G. Carrasco, H. Renaudineau and T.A. Meynard, "Analysis of Partial Power DC–DC Converters for Two-Stage Photovoltaic Systems". IEEE Journal of Emerging and Selected Topics in Power Electronics. IEEExplore Digital Library. Vol.: 7, issue: 1, March 2019; pp. 591–603.

[4] V.M. Iyer, S. Gulur, G. Gohil, and S. Bhattacharya, "An Approach Towards Extremev_S_ Fast Charging Station Power Delivery for Electric Vehicles with Partial Power Processing". IEEE Transactions on Industrial Electronics. IEEExplore Digital Library. In press.

[5] T. Kanstad, M.B. Lillholm and Z. Zhang, "Highly Efficient EV Battery Charger Using Fractional Charging Concept with SiC Devices". IEEE Applied Power Electronics Conference and Exposition (APEC'19). IEEExplore Digital Library. March 2019, Anaheim, CA, (USA); pp. 1601–1608.

[6] S. Mallangada, M.O. Badawy and Y. Sozer, "A Novel Differential Power Processing Architecture for a Partially Shaded PV String Using Distributed Control". IEEE Energy Conversion Congress and Exposition (ECCE). IEEExplore Digital Library. September 2018, Portland (USA); pp. 6220–6227.

[7] J.S. Artal-Sevil, C. Bernal-Ruiz, J. Beyza and V.M. Bravo, "Evaluation of a Thermoelectric Generation system based on Differential-Power Processing architecture under non-uniform temperature conditions" IEEE International Autumn Meeting on Power, Electronics and Computing (ROPEC'20). IEEExplore Digital Library. November 2020, Ixtapa (Mexico); pp.: 1-6.

[8] L. Chen, H. Wu, P. Xu, H. Hu and C. Wan, "A high step-down non-isolated bus converter with Partial Power conversion based on synchronous LLC resonant converter". IEEE Applied Power Electronics Conference and Exposition (APEC'15). IEEExplore Digital Library. Charlotte, NC, USA. March 2015; pp.: 1950-1955.

[9] T. Suntio and A. Kuperman, "Comments on "An efficient Partial Power Processing DC/DC converter for distributed PV architectures"" IEEE Transactions on Power Electronics. IEEExplore Digital Library. vol. 30, no. 4. April 2015; pp.: 2372.

[10] V.M. Iyer, S. Gulur, G. Gohil, and S. Bhattacharya, "Extreme Fast Charging Station Architecture for Electric Vehicles with Partial Power Processing". IEEE Applied Power Electronics Conference and Exposition (APEC'18). IEEExplore Digital Library. March 2018, San Antonio Texas (USA); pp. 659–665.

[11] F. Xue, R. Yu and A. Huang, "Fractional converter for high efficiency high power battery energy storage system". IEEE Energy Conversion Congress and Exposition (ECCE'17). IEEExplore Digital Library. Cincinnati, Ohio (USA). October 2017; pp. 5144–5150.

[12] J.S. Artal-Sevil, C. Bernal-Ruiz, J. Anzola, I. Aizpuru, A. Bono-Nuez and J.M. Sanz-Alcaine, "Partial Power Processing architecture applied to a Battery Energy Storage System" IEEE Vehicle Power and Propulsion Conference (VPPC'20). IEEExplore Digital Library. November-December 2020; Gijón (Spain) pp.: 1-6.

[13] J. Anzola, I. Aizpuru, A. Arruti, A. Alacano, R. Lopez, J.S. Artal-Sevil and C. Bernal-Ruiz, "Partial Power Processing Based Charging Unit for Electric Vehicle Extreme Fast Charging Stations". IEEE Vehicle Power

and Propulsion Conference (VPPC’20). IEEExplore Digital Library. November 2020, Gijon (Spain); pp.: 1-6.

[14] M.C. Mira, Z. Zhang, K.L. Jørgensen and A.E.M. Andersen, "Fractional Charging Converter With High Efficiency and Low Cost for Electrochemical Energy Storage Devices". IEEE Transactions on Industry Applications. IEEExplore Digital Library. Vol.: 55, issue: 6 Nov 2019; pp. 7461–7470.

[15] J.S. Artal-Sevil, V. Ballestín-Bernad, A. Coronado-Mendoza and J.L. Bernal-Agustín, “Design and Analysis of a Partial-Power Converter with an Active Power-Buffer for a Fuel Cell-based Hybrid Electric Vehicle”. IEEE Vehicle Power and Propulsion Conference (VPPC’21). IEEExplore Digital Library. Gijón (Spain), October 2021; pp.: 1-6.

[16] Y. Benomar, M. El Baghdadi, O. Hegazy, Y. Yang, M. Messagie and J. Van Mierlo, "Design and modeling of V2G inductive charging system for light-duty Electric Vehicles". International Conference on Ecological Vehicles and Renewable Energies (EVER17). IEEExplore Digital Library. April 2017. MonteCarlo (Mónaco); pp. 1–7.

[17] A. Farjah, E. Bagheri, A.R. Seifi and T. Ghanbari, "Main and auxiliary parts of battery storage, aimed to fast charging of electrical vehicles" Annual Power Electronics, Drives Systems and Technologies Conference (PEDSTC’18). IEEExplore Digital Library. February 2018; Tehran (Iran) pp.: 277-282.

[18] J.S. Artal-Sevil, V. Ballestín-Bernad, J. Anzola and J.A. Domínguez-Navarro, "High-Gain Non-isolated DC-DC Partial-Power Converter for Automotive Applications" IEEE Vehicle Power and Propulsion Conference (VPPC’21). IEEExplore Digital Library. October 2021; Gijón (Spain) pp.: 1-6.

[19] Y. Cao, M. Ngo, N. Yan, D. Dong, R. Burgos and A. Ismail, "Design and Implementation of an 18 kW 500 kHz 98.8% Efficiency High-density Battery Charger with Partial Power Processing". IEEE Journal of Emerging and Selected Topics in Power Electronics. IEEExplore Digital Library. August 2021; pp.: 1-14.

[20] K. Zheng, W. Zhang, X. Wu and L. Jing, "Optimal Control Method and Design for Modular Battery Energy Storage System Based on Partial Power Conversion". IEEE Access. IEEExplore Digital Library. Vol. 9, September 2021; pp.: 133376-133386.